Structure and Thermal Properties of PU/P(BMI–UBMI) IPNs

YUANLI CAI, ZHONGMING JIANG, DAFONG YANG, PENGSHENG LIU

College of Chemistry and Chemical Engineering, Xiangtan University, Hunan, 411105, People's Republic of China

Received 12 June 1997; accepted 30 October 1997

ABSTRACT: The preparation of polyurethane/poly(bismaleimide–urethane bismaleimide) [PU/P(BMI–UBMI)] IPNs were carried out in two steps. The two-network interaction and the morphology of PU/P(BMI–UBMI) IPNs were characterized by FTIR and TEM. The effect of the interpenetration of P(BMI–UBMI) and PU on the hydrogen bonds of N—H and the pyrolysis procedure of PU/P(BMI–UBMI) IPNs were investigated by DSC and TG. The results indicate that the interpenetration of P(BMI–UBMI) and PU reinforces the hydrogen bonding of N—H, and the incorporating of UBMI enhances the compatibility of the two networks, leading to ideal interpenetrating, which weakens the force constant of C—N—C in maleimide rings. The morphology of PU/P(BMI–UBMI) IPNs shows multiphase domains which have an obvious phase interface. The domains are connected to each other and the domain dimensions are far smaller than those of PU. The thermal weight loss shows obvious stages at different pyrolysis periods. The thermal stability of PU/P(BMI–UBMI) IPNs are much better than that of PU given the content and crosslink density of P(BMI–UBMI) in a certain range. © 1998 John Wiley & Sons, Inc. J Appl Polym Sci 68: 1689–1694, 1998

Key words: PU/P(BMI–UBMI) IPNs; hydrogen bonds; microphase separation; morphology; pyrolysis

INTRODUCTION

Polybismaleimides (PBMIs) are well known as crosslinked resins with excellent thermal stability and exhibit a similar mechanical strength to that of epoxies. However, they have a very low elongation at break and low fracture toughness because of their highly crosslinked structure.[1–5] Efforts on toughening BMI have been made for the last few decades.[6–8] Poly(bismaleimide–urethane bismaleimide) [P(BMI–UBMI)] copolymers were synthesized by incorporating the flexible chain of an ordinary polyurethane (PU) prepolymer into the backbone of the BMI by the condensation reaction of an isocyanate-teminated PU prepolymer with maleic anhydride, which shows good mechanical properties and much better thermal stability than that of the traditional PU elastomers.[9,10]

In this work, we synthesized a P(BMI–UBMI) prepolymer in *N,N′*-dimethylformamide and added the materials, which can be polymerized to form crosslinked PU, to the P(BMI–UBMI) prepolymer solution. This mixture was heated stepwise to ensure that it was reacted completely. We observed that the two crosslinked polymeric networks interpenetrated to form IPNs. The two-network interaction and the morphology of the PU/P(BMI–UBMI) IPNs were confirmed by FTIR and TEM, and the thermal properties were studied by DSC and TG. The pyrolysis procedure was investigated and is discussed in this article.

Correspondence to: Y. Cai.

Journal of Applied Polymer Science, Vol. 68, 1689–1694 (1998)
 CCC 0021-8995/98/101689-06

Table I Formulation of the Samples

Sample	Hard Segment in PU (wt %)	TMP/BD (mol)	UBMI/BMI (wt)	PU/P(BMI–UBMI) (wt)
1	36	1/3	100/0	80/20
2	36	1/3	80/20	80/20
3	36	1/3	60/40	80/20
4	36	1/3	40/60	80/20
5	36	1/3	0/100	80/20
6	36	1/3	60/40	72/28
7	36	1/3		100/0

EXPERIMENTAL

Preparation of PU/P(BMI–UBMI) IPNs

Synthesis of BMI and UBMI

The method of synthesizing BMI and UBMI is the same as in ref. 10. Poly(butylene adipate)glycol ($M_n = 1440, I_a = 0.38$). The flexible chain incorporated into the backbone of BMI to form UBMI was synthesized by the condensation polymerization of adipic acid and 1,4-butanediol (BD). The average molecular weight and acid value (I_a) were determined by traditional chemical analysis.

Preparation of PU/P(BMI–UBMI) IPNs

A solution of BMI and UBMI at various weight ratios in *N,N′*-dimethylformamide (DMF) were placed in a three-necked flask which was equipped with a stirring device, reflex condenser, thermometer and heating mantle and a constant flow of dry nitrogen. A solution of dicumyl peroxide (0.5 wt % based on the weight of BMI) was added to the reaction kettle. The temperature was maintained at 120°C until the viscosity was obviously increased before gel formation, then cooled down to room temperature. Then a mixture was added, consisting of 2,4-TDI, BD, trimethylol propane (TMP), and poly(butylene adipate)glycol ($M_n = 1400, I_a = 0.38$), to the reaction kettle and stirred at room temperature for 0.5 h. The viscous mixture was cast into a stainless-steel mold with a PTFE plate placed underneath. The solvent was removed by a vacuum at 60°C in a vacuum dryer, then maintained at 120°C at ordinary pressure for 15 h, postcured at 180°C for 1 h, and demolded after cooling. The formulations of the PU/P(BMI–UBMI) IPNs are given in Table I.

Characterization

The FTIR analysis was performed on a Perkin–Elmer FTIR-1710 spectrometer. The samples were prepared by casting the diluted reactant solution, which was dissolved in an acetone and chloroform mixed solvent, onto the PTFE mold. The solvent was removed by a vacuum at room temperature, and the mold was sealed and maintained at 120°C for 15 h. The resultant mixture was postcured at 180°C for 1 h, demolded after cooling, and then conditioned in a desiccator for at least 3 days before testing.

Morphological studies were performed using a Hitachi H-60 transmission electron microscope. The samples were stained in OsO_4 vapor and cut into sections about 100 nm thick at room temperature.

Differential scanning calorimetry (DSC) and thermogravimetric analysis (TG) were carried out on a Shimadzo TG-40 thermal analysis system. The measurement was performed in a nitrogen atmosphere at 10°C/min. The weight of the samples tested was about 6 mg, with an operating temperature range of 10–500°C.

RESULTS AND DISCUSSION

IR Analysis

The FTIR spectra of S1, S4, S5, and S7 are given in Figure 1. A summary of appropriate frequency assignments of these samples is presented in Table II.

The C—N—C bond of the unreacted maleimide was represented by the absorption peak at 1147 cm^{-1}. After curing, the intensity of the absorption peak at 1147 cm^{-1} decreased and another absorption peak was observed at 1187 cm^{-1}.[10,11]

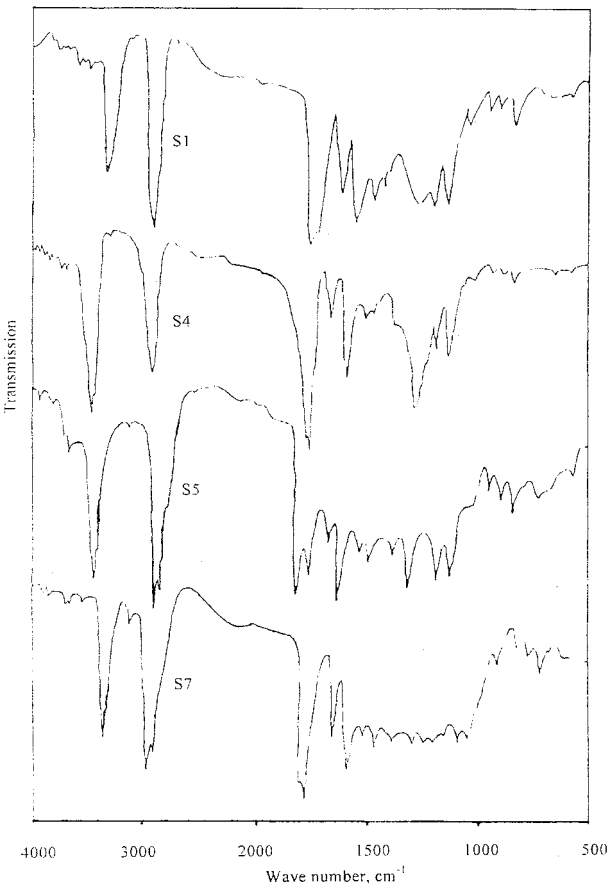

Figure 1 FTIR spectra of samples.

In the current study, the frequency of C—N—C for the PU/P(BMI–UBMI) IPNs was observed at 1184 cm^{-1} when UBMI/BMI = 0/100 and observed at 1172 cm^{-1} when UBMI/BMI = 40/60 and 100/0, which indicated that the incorporation of UBMI in P(BMI–UBMI) decreased the force constant of C—N—C in the maleimide rings. This conclusion was also confirmed by TG analysis.

The frequency of the hydrogen-bonded N—H stretching absorption peak was observed at 3337 cm^{-1} when UBMI/BMI = 100/0, while S7 was at 3337 cm^{-1} (ref. 12) and the relative intensity was lower than that of S7. This result illustrates that the hydrogen bonds of N—H are weakened by the interpenetration UBMI, which is caused mainly by the excellent compatibility of UBMI and PU and the ideal interpenetrating of the two networks, hindering the microphase separation of PU and diluting the hydrogen bonds of N—H. The relative intensity of the peak of hydrogen-bonded N—H stretching was enhanced dramatically and the frequency was observed at 3325 cm^{-1} when UBMI/BMI = 40/60, which indicates that the hydrogen bonding of N—H was reinforced due to that the crosslink density of P(BMI–UBMI) was enlarged, which was caused by enhancement of the connection of N—H with C=O, that is, the hydrogen-bond density was enlarged due to the crosslink density.

The frequency and the relative intensity of the hydrogen-bonded N—H stretching peak is similar to that of S7 when UMI/BMI = 0/100, which indicates that PBMI is not compatible with PU. It aggregates to some isolated domains which do not affect the microphase separation of PU; accordingly, it does not affect the hydrogen bonding of N—H, given the low content of PBMI.

Morphologic Studies

The TEM of S3 is given in Figure 2. The morphology of PU/P(BMI–UBMI) IPNs shows a multiphase domain structure which had an obvious phase interface. The domains are connected to each other. The result illustrates that the two networks have been interpenetrated and the aggregation of each domain is retarded by the interpenetration of the two networks. The interpenetration is not completely soluble in the molecular degree, but interfacial in each domain. Each type of segment remains aggregated, respectively, to form relatively independent domains.

Table II IR Spectral Data of Samples

Frequency (cm^{-1})				
S1	S4	S5	S7	Assignment
3321	3325	3341	3337	N—H stretching (H-bonded)
2951	2957	2952	2952	C—H stretching in CH_2
1172	1172	7784		C—N stretching in maleimide ring

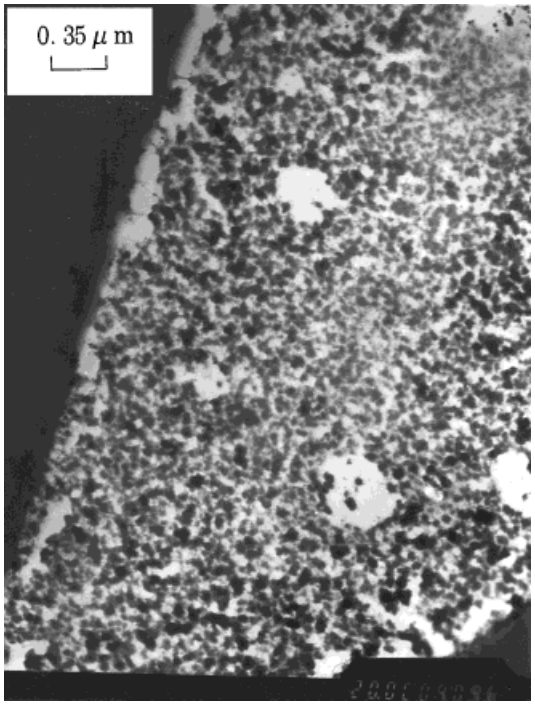

Figure 2 TEM micrograph of S3.

A summary of the domain dimensions of the samples is given in Table III. The domain dimension of S5 is 941 nm, when UBMI/BMI = 0/100, near to that of S7 (1174 nm), which confirms the conclusion deduced by IR analysis that PBMI is not compatible with PU. The introduction of PBMI to PU is similar to that of hard-plastic filling to PU using traditional blending, which has little affect on the microphase separation of PU given that the content of PBMI is low. The domain dimension of S3 is 31 nm, when UBMI/BMI = 60/40, which is far smaller than that of S7. The result illustrates that the incorporation of PBMI in P(BMI–UBMI) decreases the crosslink density of P(BMI–UBMI) and reinforces the compatibility of the two networks, leading to ideal interpenetration. The interlocking of the two networks enhances the mutual entanglement and retards the aggregation of each segment. The domain dimension of S2 is 113 nm when UBMI/BMI = 80/20, which was caused by the excellent interpenetration of the two networks and the lower crosslink density of the P(BMI–UBMI) copolymer.

Table III Domain Dimensions of Samples

Sample	2	3	5	7
Domain dimensions (nm)	113	31	941	1174

Thermal Properties Studies

The DSC curves of S2, S3, S6, and S7 are given in Figure 3, and the temperatures of each endothermal peak are given in Table IV.

The endothermal peak at T_1 is that of the destruction of hydrogen bonds and that at T_2 belongs to the pyrolysis of urethane.[12,13] A endothermal peak is observed at a high temperature of about 400°C for IPNs but is not observed in that of PU; thus, this peak is deduced as the endothermal peak of the pyrolysis of maleimide rings.[10]

By investigating the endothermal peaks of hydrogen-bond destruction, a conclusion, deduced by FTIR analysis, can be confirmed that the interpenetration of P(BMI–UBMI) and PU enhanced the hydrogen bonding given a certain content of UBMI/BMI of P(BMI–UBMI), but too much UBMI incorporation in P(BMI–UBMI) and too much content of P(BMI–UBMI) can dilute the hydrogen bonds and weakens them so they can be easily destroyed.

The T_2's of the IPNs are higher and the peak areas are larger than those of PU. This is caused mainly by interpenetration and mutual entanglement, which enhances the interaction of each segment, including PU segments and maleimide rings; accordingly, more energy should be provided to destroy these segments, that is, the cohesive energy density (CED) of the PU hard-segment domains increased due to the incorporation of P(BMI–UBMI). The enthalpy for the pyrolysis of urethane should be larger than that of PU.

By analyzing T_3 in Table IV, a higher content or crosslink density of P(BMI–UBMI) leads to higher temperature and a larger enthalpy of the pyrolysis of maleimide rings. This is caused mainly by the enlargement of maleimide rings and better microphase separation of P(BMI–UBMI). The CED of maleimide domains was decreased by the introduction of PU segments; accordingly, the pyrolysis temperature moves to that of urethane.

The TG curves of S2, S3, S6, and S7 are given in Figure 4. It is easily observed that the weight loss, especially that of the IPNs, shows obvious stages at different periods of the pyrolysis proce-

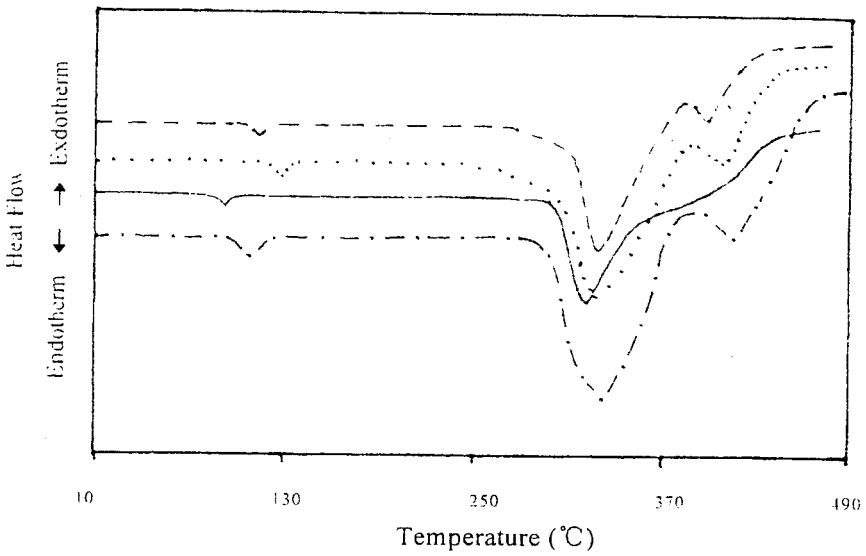

Figure 3 DSC for samples: (——) S7; (— · —) S6; (----) S2; (. . . .) S3.

dure, that is, the speed of weight loss is various at the different pyrolysis periods. A summary of the start temperature (T_e) and weight loss (ΔW) of each stage are given in Table V.

It can be deduced by DSC analysis that the first stage of weight loss is the pyrolysis procedure of urethane, which consists of a hard segment in PU and a flexible urethane segment in UBMI; the second stage is the pyrolysis procedure of the ester in the soft segment in PU and UBMI and the further degradation of the urethane.[14] The start temperatures of the weight loss of IPNs are higher and the weight loss of IPNs are lower than those of PU at 300–400°C. This result indicates that the incorporation of P(BMI–UBMI) retards the pyrolysis of PU segments.

The maleimide rings start to pyrolyze at the beginning of the third stage,[10] that is, the weight loss at the third stage is the total result of the pyrolysis procedure of all segments. It can be easily observed from the TG curves at the same temperature at the third stage that the weight loss of each sample is S6 < S3 < S7 < S2; the weight loss decreases as the content of maleimide rings increased. However, too large UBMI incorporated in P(BMI–UBMI) improves the pyrolysis speed due to the force constant of C—N—C weakened by the UBMI incorporation deduced by IR analysis. The result is consistent with the conclusion deduced by the DSC analysis.

Table IV Temperatures of Endothermal Peaks

Sample	2	3	6	7
T_1	114.2	122.8	108.9	101.7
T_2	320.0	323.9	331.1	317.5
T_3	396.4	410.4	415.6	

CONCLUSIONS

The following conclusions have been drawn from this study: The interpenetration of P(BMI–UBMI) and PU obviously affects the hydrogen bonding of N—H. The UBMI/BMI of P(BMI–UBMI) is one of the key factors influencing the hydrogen bonding. Hydrogen bonds were enhanced dramatically for UBMI/BMI in the range of 40/60 to 60/40. The force constant of C—N—C in maleimide rings is weakened by the incorporation of UBMI in P(BMI–UBMI).

The morphology of PU/P(BMI–UBMI) IPNs shows a multiphase domain structure from which was observed, evidently, phase interface and the domains connected to each other. The domain dimensions of IPNs are far smaller than those of PU given a certain content and crosslink density of P(BMI–UBMI). The result illustrates that the two networks have been interpenetrated.

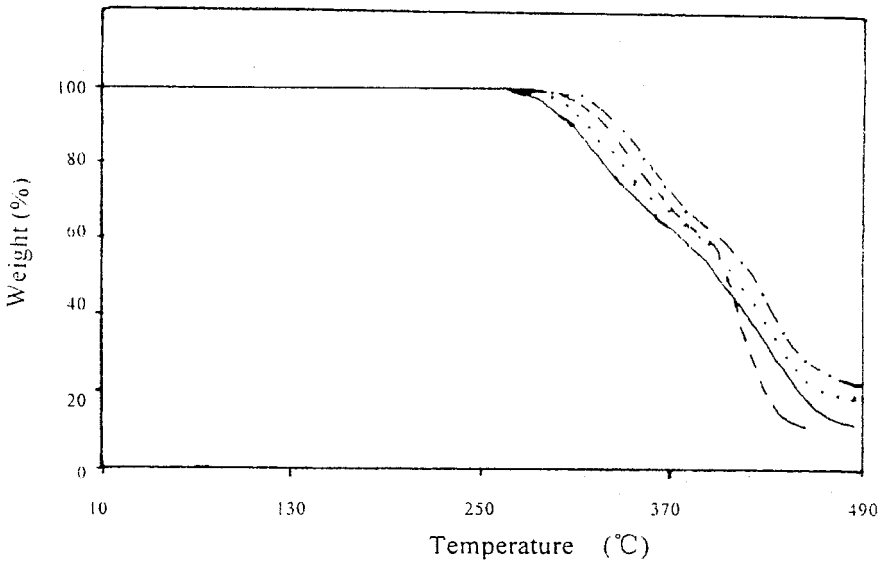

Figure 4 TG analysis of samples: (——) S7; (— · —) S6; (----) S2; (. . . .) S3.

The pyrolysis procedure of the PU/P(BMI–UBMI) IPNs shows obvious stages. The interpenetration of the two networks retards the destruction of hydrogen bonds and the pyrolysis of urethane, that is, PU/P(BMI–UBMI) IPNs show better thermal stability than that of PU.

Table V TG Analysis Results

	Sample			
Variable	2	3	6	7
T_{01}	306.8	291.1	313.8	262.7
T_{e1}	343.7	303.9	367.1	345.9
ΔW_1 (%)	−18.5	−22.7	−28.7	−27.5
T_{02}	343.7	330.9	367.1	345.9
T_{e2}	390.9	385.5	405.4	467.6
ΔW_2 (%)	−20.6	−12.9	−13.9	−58.1
T_{03}	390.9	385.5	405.4	
T_{e3}	455.4	464.3	427.8	
ΔW_3 (%)	−46.2	−42.9	−34.1	
$\Sigma\Delta W$ (%)	−84.8	−78.5	76.7	−85.6

T_0 and T_e, the start temperature and the end temperature, respectively, at each stage; ΔW and $\Sigma\Delta W$, the weight loss at each stage and the total weight loss at the end of the third stage, respectively; 1, 2, and 3, the first, second, and third stage, respectively.

REFERENCES

1. I. K. Varma, G. M. Fohlen, and J. A. Parker, *Macromol. Sci. Chem. A,* **19,** 209 (1983).
2. A. V. Galanti and D. A. Scola, *J. Polym. Sci. Polym. Chem. Ed.,* **19,** 451 (1981).
3. J. E. White, M. D. Scaia, and D. A. Snider, *J. Polym. Sci. Polym. Chem. Ed.,* **22,** 589 (1984).
4. J. E. White, M. D. Scaia, and D. A. Snider, *J. Appl. Polym. Sci.,* **29,** 891 (1984).
5. K. N. Ninan, K. Krishnan, and Mathew, *J. Appl. Polym. Sci.,* **32,** 6033 (1986).
6. J. P. Pan, G. Y. Shiau, and K. M. Chen, *J. Appl. Polym. Sci.,* **44,** 467 (1992).
7. S. Jakeda and H. Kakiuchi, *J. Appl. Polym. Sci.,* **35,** 1351 (1988).
8. N. Suzuki, A. Nagai, M. Suzuki, and A. Takahashi, *J. Appl. Polym. Sci.,* **44,** 1807 (1992).
9. D. C. Liao and K. H. Hsieh, *J. Polym. Sci. Part A Polym. Chem.,* **32,** 1665 (1994).
10. D. C. Liao, K. H. Hsieh, and S. C. Kao, *J. Polym. Sci. Part A Polym. Chem.,* **33,** 481 (1995).
11. C. Digiulio, M. Gautier, and B. Jasse, *J. Appl. Polym. Sci.,* **29,** 1771 (1991).
12. V. W. Srihatrafrimuk, *J. Macromol. Sci. Phys. B,* **15,** 267 (1978).
13. Y. L. Cai, Z. M. Jiang, and P. S. Liu, *Polym. Mater. Sci. Eng.,* **13**(3), 67 (1997).
14. Y. L. Cai, Z. M. Jiang, and P. S. Liu, *Polym. Mater. Sci. Eng.,* **13**(4), 120 (1997).